# Investigating the effect of neoclassical tearing modes on fast ions in ASDEX Upgrade: measurements and modelling

A. S. Jacobsen[1], B. Geiger[1], R. J. Akers[2], J. Buchanan[2], K. G. McClements[2], A. Snicker[3], V. Igochine[1], D. Meshcheriakov[1], M. Salewski[4], M. Dunne[1], E. Poli[1], P. A. Schneider[1], G. Tardini[1], A. Jansen van Vuuren[1], M. Weiland[1]

the ASDEX Upgrade team and the EUROfusion MST1 team*

[1] *Max-Planck-Institut für Plasmaphysik, D-85748 Garching, Germany*

[2] *CCFE, Culham Science Centre, Abingdon OX14 3DB, United Kingdom*

[3] *Department of Applied Physics, Aalto University, FI-00076 Aalto, Finland*

[4] *Department of Physics, Technical University of Denmark, DK-2800 Kgs. Lyngby, Denmark*

## Introduction

Neoclassical tearing modes (NTMs) are MHD instabilities which can form at rational surfaces in tokamak plasmas. They appear at high plasma pressure and limit the achievable plasma performance by degrading the confinement. Large NTMs can even lead to plasma disruptions. NTMs are characterized by $(m,n)$, their poloidal and toroidal mode numbers, respectively. It has previously been observed that NTMs cause losses of fast ions [1, 2, 3]. Here, these studies are expanded by investigating the internal transport of confined fast ions.

## Experimental observations

The fast-ion $D_\alpha$ (FIDA) spectroscopy diagnostic is a charge-exchange diagnostic measuring the Doppler shift of deuterium Balmer alpha radiation. In order to have a sufficiently strong source of neutral particles, the ASDEX Upgrade FIDA system looks at one of the 60 keV neutral beams used for heating. The system consists of five in-vessel lenses, oriented such that each observes the plasma from a different angle. This is important for calculating the fast-ion distribution function directly from the measurements using velocity-space tomography[4, 5]. From each lens, a number of lines-of-sight are oriented in a fan-like pattern crossing the neutral beam. This enables the FIDA diagnostic to measure at different radial locations. The measurement regions are defined by the overlap of a line-of-sight and the neutral beam, and are of the order of a few centimetres. Figure 1 shows time traces from the ASDEX Upgrade discharge analysed in this paper. The top panel shows the neutral beam injection (NBI) and electron cyclotron resonance heating (ECRH) power. The ECRH power is constant throughout the discharge while the NBI

*See author list of "H. Meyer et al 2017 Nucl. Fusion 57 102014"

heating is ramped from 5 MW to 15 MW. This is done in order to purposely trigger an NTM. The second panel shows a magnetic spectrogram where the mode activity can be seen. The third panel shows the plasma stored energy and the electron density in the core of the plasma. The fourth panel shows the fast-ion signal from the lines-of-sight of one of the lenses of the FIDA diagnostic. The parts of the spectra dominated by the fast ions are integrated, normalised to the beam emission signal and plotted as a function of time and radius, here given by $\rho_t$ the square-root of the normalized toroidal flux. From $t = 2.4$ s to $t = 2.58$ s fishbones can be seen in the magnetic spectrogram. No strong effects on the fast ions or the plasma are observed. At $t = 2.58$ s a fishbone triggers a $(2,1)$ NTM. This causes a decrease of stored energy, core density and fast-ion signal. At $t = 2.7$ s the observed frequency of the $(2,1)$ NTM goes to 0 as the mode stops rotating and locks to the error field. Neither the plasma nor the fast-ion signals recover, despite the increased heating, and the plasma disrupts at $t = 3.27$ s. The FIDA signal depends on the local fast-ion distribution as well as the background plasma, and forward modelling of the signal is necessary in order to determine whether the observed drop in FIDA signal is due to changes in plasma profiles or to fast-ion transport. Such modelling of synthetic spectra has been carried out using the FIDA forward model FIDAsim[6] and a fast-ion distribution function from TRANSP/NUBEAM[7], and it cannot explain the observed drop in FIDA signal. It should here be noted that TRANSP/NUBEAM assumes a toroidally symmetric equilibrium. As mentioned earlier, it is possible to calculate the fast-ion distribution function directly from the measurements using velocity-space tomography. This is done here for $t = 2.6$ s and $t = 2.7$ s near the centre of the plasma at $\rho_t = 0.1$. The results are shown in figure 2. A significant drop in the fast-ion distribution is observed after the (2,1) NTM has been present for 100 ms. The tomography is computed assuming a smooth and non-negative solution.

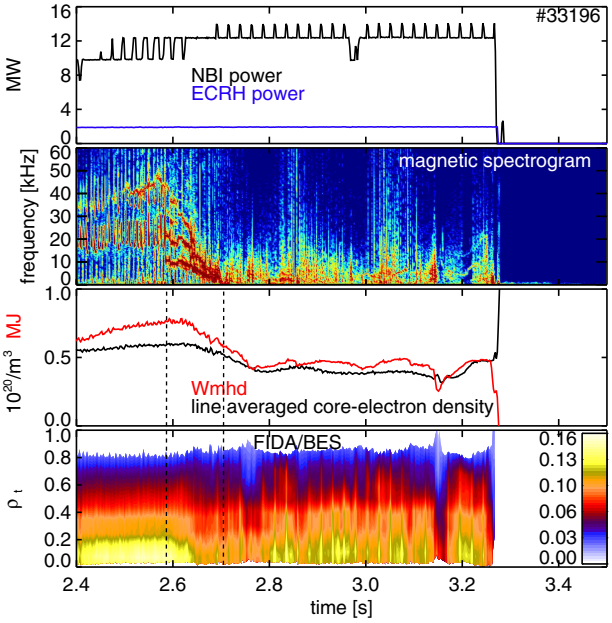


Figure 1: *Time traces of ASDEX Upgrade discharge 33196 showing the effect on the plasma and the fast ions of a large (2,1) NTM.*

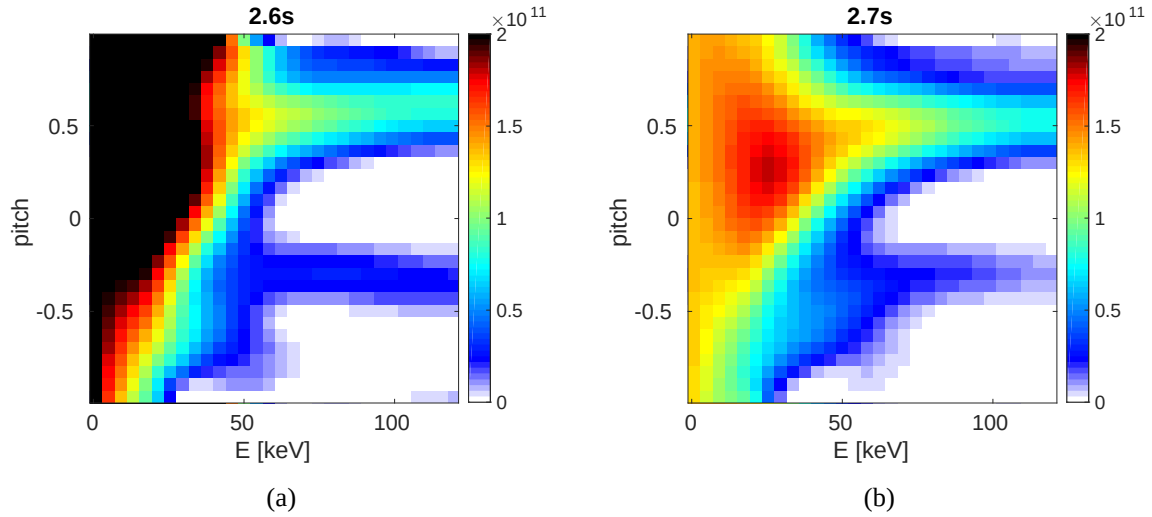


(a) (b)

Figure 2: *Fast-ion distribution functions in units of [ions/keV/pitch/cm$^3$] calculated using velocity-space tomography. (a) At the onset of the (2,1) NTM. (b) After the (2,1) NTM locks.*

**NTM modelling**

It is possible to match the forward modelled FIDA signal to the measured one using a TRANSP/NUBEAM distribution that considers an ad-hoc anomalous fast-ion diffusion. However, ideally the fast-ion distribution function should be simulated taking into account the fast-ion transport induced by the magnetic field perturbation itself, and not just the changing plasma profiles and an unphysical anomalous diffusion. This is done here using the full-orbit code LOCUST[8], which can calculate the fast-ion distribution function from a realistic ionization profile, taking into account collisions, a realistic tokamak geometry as well as magnetic perturbations, for $t = 3.0$ s where the NTM is locked. The perturbation due to the NTM is calculated as a perturbed magnetic vector potential, $\tilde{\mathbf{A}}$, and it is assumed that the perturbation in the magnetic vector potential is along the background magnetic field, following the procedure used in [9]:

$$\tilde{\mathbf{A}} = \alpha \mathbf{B}\,. \tag{1}$$

The perturbed magnetic field, $\tilde{\mathbf{B}}$, is then calculated as the curl of the perturbed magnetic vector potential. $\alpha$ in equation (1) is defined as

$$\alpha = \sum_{m,n} \alpha_{m,n} \cos(m\theta - n\phi)\,, \tag{2}$$

where $\alpha_{m,n}$ are radial functions which describe the position, shape and amplitude of the perturbation for a given set of mode numbers, $\theta$ is the straight-field-line poloidal angle and $\phi$ is the toroidal angle. The size of the mode is estimated from electron temperature variations measured

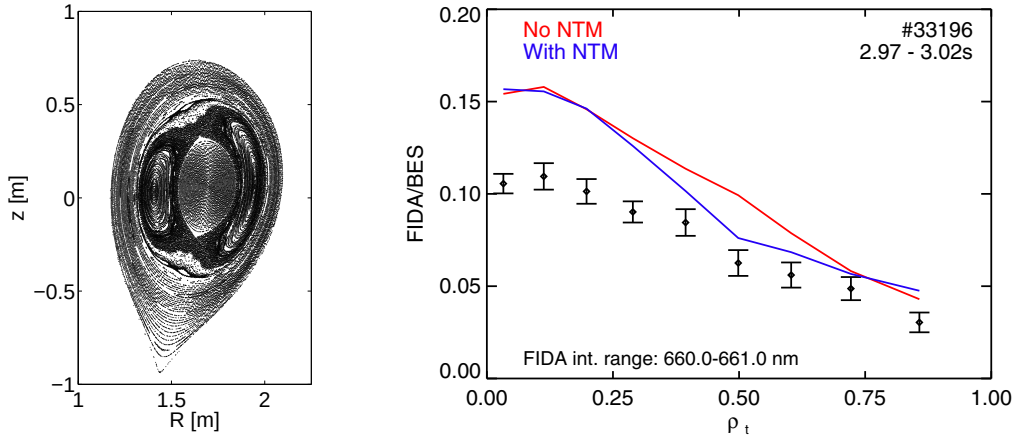


(a) (b)

Figure 3: *(a) Poincare plot of strong (2,1) NTM. (b) Measured and synthetic radial FIDA profiles. Including the NTM in the simulation improve the match to the measured profile.*

by the electron cyclotron emission diagnostic. Figure 3a shows a Poincare plot of a large (2,1) NTM generated using LOCUST. The perturbation is so large that the magnetic field close to the (2,1) island becomes stochastic. The fast-ion distribution function simulated including this perturbation is used with FIDAsim to calculate synthetic spectra. A radial profile is calculated from these and shown in figure 3b (blue) together with a simulation with an axi-symmetric equilibrium (red) and the measured profile (black). Including the (2,1) NTM in the simulation improves the match between simulation and measurement around mid-radius. However, there is still a discrepancy in the centre of the plasma. The hypothesis is that this is caused by a (1,1) kink mode, which can couple toroidally to (2,1) modes in tokamaks. However, identifying this in the experiment is difficult since the NTM is locking. Work on including this (1,1) kink mode in the simulation is ongoing.

## Acknowledgement

This work has been carried out within the framework of the EUROfusion Consortium and has received funding from the Euratom research and training programme 2014-2018 under grant agreement No 633053. The views and opinions expressed herein do not necessarily reflect those of the European Commission.

## References

[1] H. E. Mynick, Physics of Fluids B **5**, 1471 (1993)
[2] M. García-Muñoz *et al.*, Nuclear Fusion **47**, L10-L15 (2007)
[3] E. Poli *et al.*, Physics of Plasmas **15**, 032501 (2008)
[4] M. Salewski *et al.*, Nucl. Fusion **54**, 023005 (2014)
[5] A. S. Jacobsen *et al.*, Plasma Phys. Control. Fusion **58**, 045016 (2016)
[6] W. W. Heidbrink *et al.*, Commun. Comput. Phys. **10**, 716-741 (2011)
[7] A. Pankin *et al.*, Computer Physics Communications **159**, 157-184 (2004)
[8] R. J. Akers *et al.*, 39th EPS Conference & 16th Int. Congress on Plasma Physics, P5.088, (2012)
[9] E. Hirvijoki *et al.*, Computer Physics Communications **183**, 2589-2593 (2012)